AIAA-99-0944

AN AIR BEARING BALANCE WITH 1-DOF SPIN CAPABILITY

J.C. Magill*, K.R. McManus†, M.R. Malonson‡, J.A. Ziehler‡, and M.F. Hinds§
Physical Sciences Inc.
Andover, MA 01810

Abstract

This paper describes the development and testing of a one degree-of-freedom air bearing balance for dynamic wind tunnel testing. The balance permits test articles to spin without friction while making measurements of loads. Five load components are measured by sensing pressures in the air bearing film. The sixth component - rolling torque - is determined by sensing the current needed by the brushless spin motor to maintain a given rotation rate. The balance is also fitted with a novel auxiliary air delivery system which delivers air to the test model for pneumatic actuators or reaction control jets. The paper describes the design of the balance and preliminary testing in Physical Sciences Inc.'s (PSI's) automated calibration facility. Calibration results indicate that the blaance responds linearly to applied loads. However, because it is impossible to manufacture a bearing with perfect uniformity, the balance must be calibrated as a function of bearing roll angle.

Introduction

This paper describes the design and testing of a one degree-of-freedom (1-DOF) air bearing balance. The balance is intended for use in testing spinning projectile or missile models, as well as for making measurements on aircraft models mounted free-to-roll. This work is a continuation of the feasibility demonstration reported earlier[1] and is part of a larger effort to develop the mounting and sensing capabilities necessary for wind tunnel Virtual Flight Testing (VFT).[2]

An air bearing consists of two elements, one fixed and one floating, separated by a thin film of high pressure air. Film thicknesses are typically 15 to 25 µm, or 0.0007 to 0.001 in. Air enters the film through a set of injection orifices as shown in Figure 1. Because the surfaces are not in contact, the bearing presents very little friction. As a load normal to the film is applied to the floating element, the film thickness decreases. This reduces the mass flow through the film because the film flow resistance increases. With the mass flow reduced, the pressure drop through the orifice is smaller and the air in the film is thus at a higher pressure. The increase in pressure supports the applied load. The bearing design process essentially consists of matching the film and orifice resistances to achieve the desired performance. The maximum load capacity for an air bearing is usually defined as the load for which the film height changes 50%. The film typically acts like a stiff linear spring over this range.

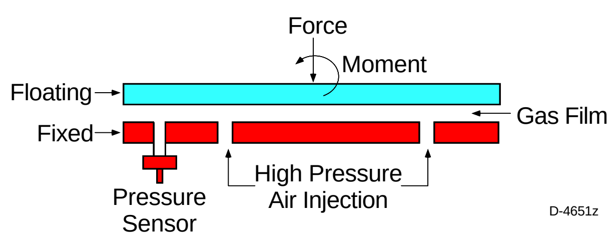

Figure 1. The air bearing balance concept.

Because the pressure in the film supports the applied loads, the applied loads may be determined by measuring the film pressures. If two bearing surfaces are arranged to oppose one another and support bi-directional loads, then small differences in pressure between the two films can be measured with low-range differential sensors to determine the loads. Thus a very sensitive load sensor can be made from very stiff bearings. This is a significant advantage over deflection measurement techniques such as strain gage or LVDT balances, where increased sensitivity requires reduced stiffness. High stiffness is required to achieve a high natural frequency and enable dynamic load measurement.

The air bearing balance was initially used by Haldeman and Weinberg[3] to test spinning models. Though the principal of operation was successfully demonstrated, their balance was unable to make high

* Principal Scientist, Member AIAA
† Principal Research Scientist, Member AIAA
‡ Senior Research Scientist
§ Senior Programmer

Copyright @ 1998 by Physical Sciences Inc. Published by the American Institute of Aeronautics and Astronautics, Inc. with permission.

Report Documentation Page

Form Approved
OMB No. 0704-0188

Public reporting burden for the collection of information is estimated to average 1 hour per response, including the time for reviewing instructions, searching existing data sources, gathering and maintaining the data needed, and completing and reviewing the collection of information. Send comments regarding this burden estimate or any other aspect of this collection of information, including suggestions for reducing this burden, to Washington Headquarters Services, Directorate for Information Operations and Reports, 1215 Jefferson Davis Highway, Suite 1204, Arlington VA 22202-4302. Respondents should be aware that notwithstanding any other provision of law, no person shall be subject to a penalty for failing to comply with a collection of information if it does not display a currently valid OMB control number.

1. REPORT DATE **1998**	2. REPORT TYPE	3. DATES COVERED **00-00-1998 to 00-00-1998**

4. TITLE AND SUBTITLE **An Air Bearing Balance with 1-DOF Spin Capability**	5a. CONTRACT NUMBER
	5b. GRANT NUMBER
	5c. PROGRAM ELEMENT NUMBER
6. AUTHOR(S)	5d. PROJECT NUMBER
	5e. TASK NUMBER
	5f. WORK UNIT NUMBER
7. PERFORMING ORGANIZATION NAME(S) AND ADDRESS(ES) **Physical Sciences Inc,20 New England Business Center,Andover,MA,01810**	8. PERFORMING ORGANIZATION REPORT NUMBER
9. SPONSORING/MONITORING AGENCY NAME(S) AND ADDRESS(ES)	10. SPONSOR/MONITOR'S ACRONYM(S)
	11. SPONSOR/MONITOR'S REPORT NUMBER(S)

12. DISTRIBUTION/AVAILABILITY STATEMENT
Approved for public release; distribution unlimited

13. SUPPLEMENTARY NOTES
The original document contains color images.

14. ABSTRACT
see report

15. SUBJECT TERMS

16. SECURITY CLASSIFICATION OF:			17. LIMITATION OF ABSTRACT	18. NUMBER OF PAGES	19a. NAME OF RESPONSIBLE PERSON
a. REPORT **unclassified**	b. ABSTRACT **unclassified**	c. THIS PAGE **unclassified**		**9**	

frequency measurements. In the mid-80's when the work was performed, the available pressure sensors were too large to be placed inside of the balance itself. The sensors were located outside of the tunnel and connected to the air bearing by long tubes, resulting in a settling time of many seconds.

Advancements in microscale fabrication technologies make possible the use of much smaller sensors installed inside of the air bearing itself, making the air bearing balance a very capable dynamic load sensor. This and other advancements were described in a previous paper.[1] The work described herein represents a maturing of air bearing balance design.

The following sections describe the requirements used for the present 1-DOF bearing design and give an overview of the design process and issues. Later sections describe the calibration and testing of the balance in an automated pneumatic calibration rig.

Bearing Design

The 1-DOF air bearing balance was designed to fulfill the following requirements:

1. Steady load measurement capability for 750 lb sideforce or lift and 150 lb thrust. Load measurements will be made using pressure measurements in the gas film.

2. Measurement of unsteady loads with magnitudes of 5% of the steady loads at up to 800 Hz.

3. Integral spin motor capable of spinning models as high as 20,000 rpm. Spin motor current measurements will be used to sense rolling moment.

4. Angular position and velocity measurement.

5. Auxiliary air supply of 1 lbm/s at 2000 psig.

The bearing assembly consists of a journal bearing, which will bear the radial load, and a double-acting thrust bearing to carry the thrust/drag loads. Figure 2 shows how the bearing surfaces are arranged. The entire assembly is shown in Figure 3. The journal bearing consists of a pair of gas bearing separated to carry large moment loads. The thrust and journal gas bearings were designed with the aid of computer models of the gas film fluid dynamics.[4-7] The thrust bearing model and resulting designs were validated experimentally. Mathematical models of bearing dynamics predicted stability properties of the bearings.[8,9]

The primary design objective was to determine the film size, orifice type and size, and supply pressure necessary to support the required loads. Modeling codes implemented in MATLAB can calculate the pressure distribution over the bearings and can integrate the distribution to determine the bearing load capacity. Once a design had been chosen the pressure distribution

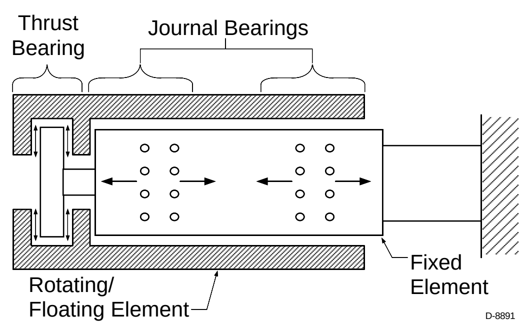

Figure 2. Arrangement of bearing surfaces.

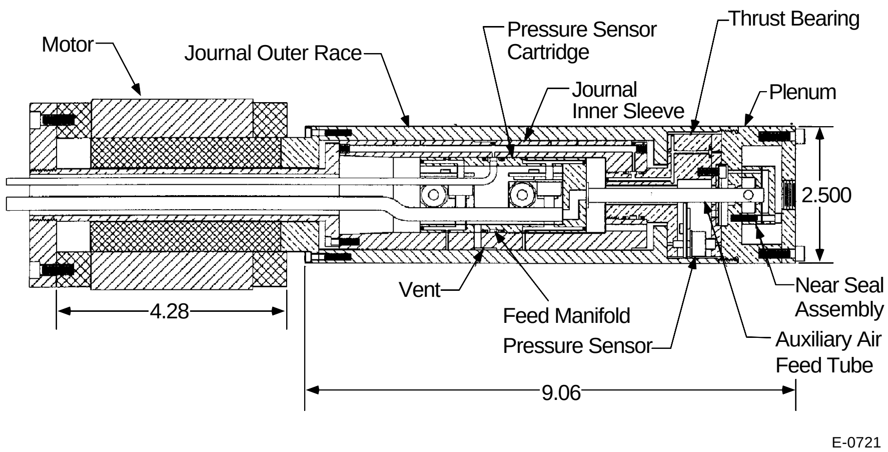

Figure 3. 1-DOF air bearing balance assembly.

calculations were used to determine the location of the pressure sensors in the bearing. The design process weighed competing requirements such as load capacity, overall dimensions, and dynamic stability.

A stability analysis of the bearings showed that the most prudent choice of compensation techniques for this particular bearing is the inherent compensation method. This results from the need to support a high load with a geometrically constrained bearing. In an inherently compensated bearing, orifices are straight cut holes. This is in contrast to orifice or groove compensation, often used in commercial bearings, which have circular or groove recesses surrounding the orifices. Film height was determined by manufacturing tolerances and journal deflection allowances. Overall dimensions were chosen from the geometric constraints. Constraining the flow to be laminar, the supply pressure and orifice diameter were chosen. Finite element stress analysis was performed using the software package ALGOR to verify that the components would not fail or deform beyond the gap height under the expected loads. The predicted load capacities and overall dimensions for the final design are shown in Table 1, along with anticipated subsystem performance specifications.

.The material for all components incorporating bearing surfaces is 17-4PH stainless steel. The bearing surfaces are coated with Diamond Black^{TM}, a boron carbide coating 2 µm thick. This coating has a hardness of 93 Rockwell C and reduces the friction coefficient between the surfaces. The coating will prevent damage to the bearing surface during assembly and setup or in the event of contact between surfaces while the bearing is spinning.

Sensor Cartridges

Pressure sensors housed within the fixed elements will measure the forces and moments from the pressure taps shown in Figure 4. Three of these are on the thrust bearing. The remaining four are positioned to measure orthogonal differences in pressure at two axial locations on the journal. Differences in each pair of aligned sensors represent moments. Common components of pressure difference in two aligned sensors yields radial loads. Three sensors are used on the thrust bearing because its pressure distribution will vary circumferentially if a moment is applied to the journal.

The sensors for measuring pressure differentials on the bearing surfaces are IC SENSORS Model 32, which are housed in a compact TO-8 package (0.5 in. diam). The sensor and its associated support electronics are shown in Figure 5. The sensors measure differential pressures in several ranges while withstanding common mode pressures up to 500 psig. The sensors have a combined linearity and hysteresis error of 0.15% f.s. These sensors, along with their associated electronics, are mounted to a 1.0 x 0.5 in. circuit board.

For measuring pressure differentials on the journal bearing, two pairs of these sensor assemblies are mounted within a cylindrical aluminum cartridge as shown in Figure 6. The sensor assemblies are oriented at a 90 deg angle relative to each other to measure differentials in both the vertical and horizontal directions. During assembly, journal sensor cartridges are inserted into the motor-mount end of the journal sleeve, and the O-ring sealed ports are aligned to mating pressure taps drilled radially in the journal sleeve.

Table 1. Design Targets and Final Design Performance Predictions

	Target	Final Design
Overall length		
with motor	---	14 in.
without motor	8.5 in.	9 in.
Bearing OD	2.5 to 3 in.	2.5 in.
Motor OD	3 in.	3.5 in.
Maximum radial load		
with motor (structurally limited)	750 lb	250 lb
without motor (bearing limited)	750 lb	640 lb
Maximum thrust load	150 lb	150 lb
Maximum motor torque	---	2 ft-lb
Maximum spin rage	20,000 rpm	20,000 rpm
Auxiliary flow capacity	1 lbm/s @ 2000 psig	0.41 lbm/s @ 2000 psig

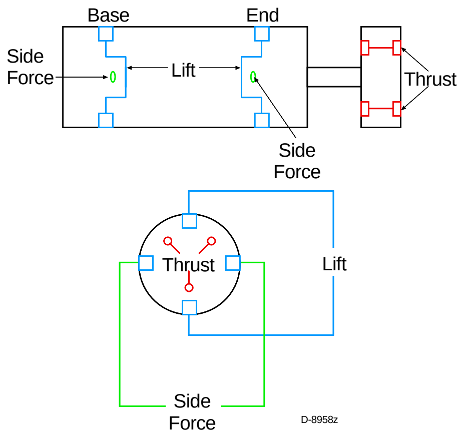

Figure 4. Placement of pressure sensors for five component load sensing.

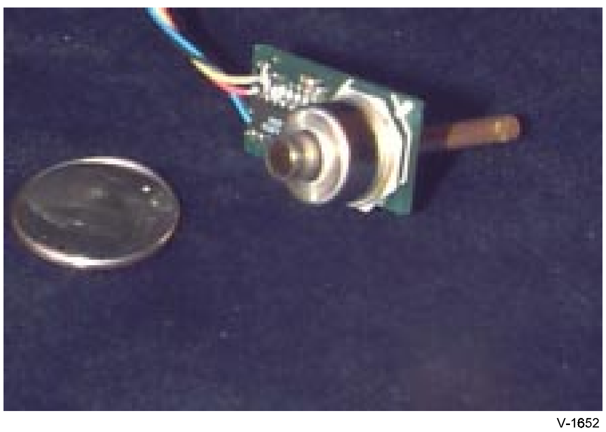

Figure 5. Model 32 pressure sensor with support electronics.

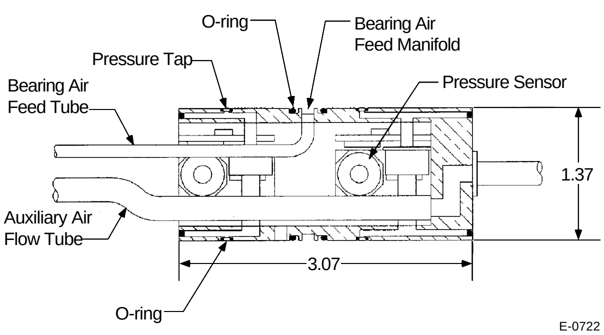

Figure 6. Journal bearing pressure sensor cartridge.

For the thrust bearing, the same sensor and board assembly is used but the sensors are not installed in cartridges. Instead, they reside in the gap between fixed element plates and are sealed to the plates.

Auxiliary Air System

One of the requirements of the 1-DOF bearing is the ability to provide auxiliary air to the model at 2000 psi pressure at a flow rate of up to 1 lb per second. A tube from the sting support will carry air which feeds a plenum at the far end of the thrust bearing. We chose a 1/4 in. OD stainless tube (0.18 in. ID) to carry this flow. This is the largest tube which can fit through the journal bearing sensor cartridges and through the necked-down portion of the thrust bearing. Flow rate calculations using adiabatic compressible flow relations show that such a tube can carry 0.81 lb per second of air without choking. However, the pressure drop at that flow rate would be 1200 psi from the source to the plenum, which is unacceptable. Assuming we want the pressure drop between the source and the plenum to be no more than 10% (1800 psi in plenum), the maximum flow rate through the supply tube is about 0.4 lb per second.

The stationary supply tube must feed a rotating plenum, without adding any friction to the rotating bearing or any axial loads to the bearing which would add an error to the thrust load measurement. To accomplish this, we used a “double near seal” approach (see Figure 7). The supply tube protrudes from the thrust bearing disk into a cavity within the plenum. A near-seal is formed by a sharp edged hole in each wall of the cavity which closely surrounds the supply tube at both ends of the cavity. The double near seal is necessary because the supply tube must not terminate inside the high pressure supply cavity. Otherwise, a large thrust load is produced. Air enters the supply tube through a pair of opposing holes on the sides of tube so than no net force is produced by the auxiliary air flow. Holes in the cavity feed air to the plenum, while the double near seal allows a small amount of air to leak equally out both ends of the cavity - thereby avoiding any contact load between the supply tube and the plenum. Notice that every surface exposed to a high pressure is balanced by an opposing surface and that all air is fed through opposing radial holes, so that no net load results from the auxiliary air system. The leaking air is vented into the interior of the journal along with the vented air from the bearing injection ports.

Spin Motor

A brushless motor at the base of the bearing will impart spin to test models. The motor is capable of producing torques greater than 2 ft-lb (24 in.-lb) and can operate at spin rates up to 20,000 rpm. An encoder inside the motor provides angular position and velocity measurements. A motor current sensor will provide

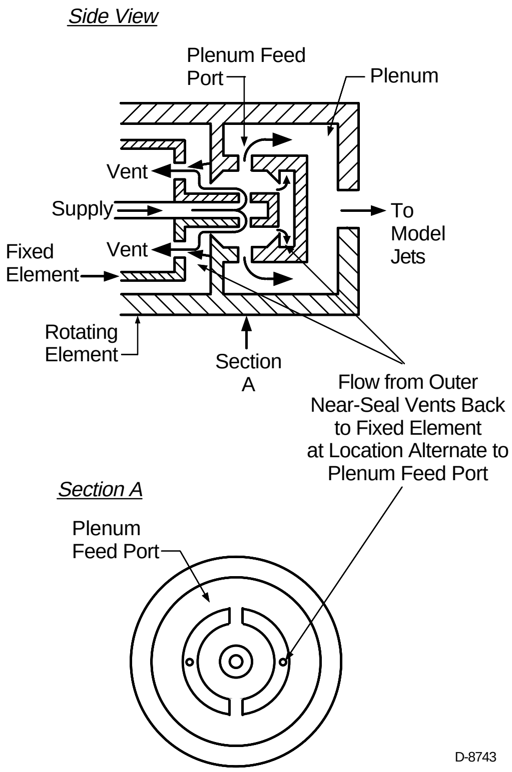

Figure 7. Auxiliary air flow system.

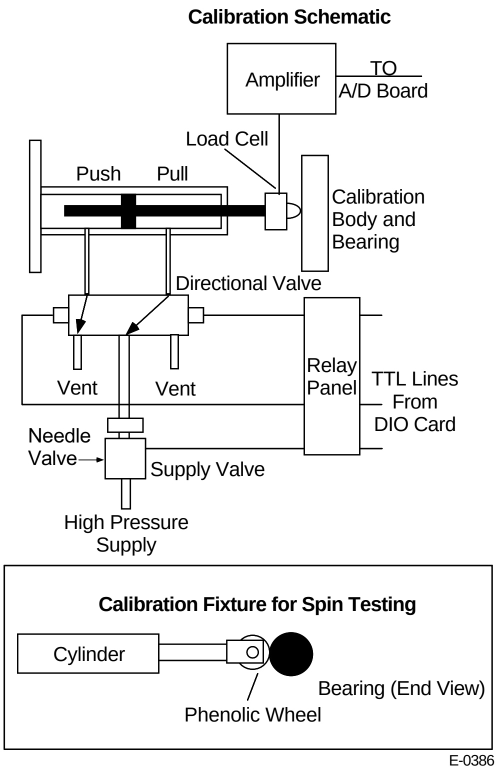

Figure 8. Calibration system schematic.

motor torque measurement signals which will be used as a measure of motor torque. The motor has a diameter slightly larger than that of the bearing but can be removed as necessary to meet testing requirements.

Calibration Facility

A fully automated air bearing balance calibration stand has been assembled at PSI. The facility is capable of applying calibration loads to both static and spinning bearings. As shown in Figure 8, calibration loads are applied using pneumatic cylinders. Loads are applied to a cylindrical calibration body that surrounds the bearing. Loads are then transmitted to the bearing itself exactly as they will be when a model, rather than the calibration body, is attached.

A calibration computer controls the loading process such that a schedule of applied loads can be specified and then automatically applied by the system. Calibration loads are measured using precision load cells. The computer is equipped with an analog data acquisition card that samples signals from both the load cells and the air bearing. Data are recorded for subsequent calibration matrix computation.

Each cylinder is fitted with a device to apply loads in only the direction along the cylinder axis. For calibrations without spin, the loads are applied through a rounded button, greased to prevent the transmission of off-axis loads through friction. For calibration of the spinning bearing, loads are applied through a phenolic wheel. It is possible, with the wheel, to apply forces parallel to the wheel axle, but these can be minimized by lubricating the surface of the wheel.

The calibration system frame is constructed from extruded aluminum beams. The five load cells/ pneumatic cylinders can be arranged to apply thrust, vertical and horizontal forces, and vertical and horizontal moments as shown in Figure 9. The thrust cylinder is capable of applying 300 lbs while the other four can apply up to 500 lbs.

Figure 10 is a photograph of the assembled calibration rig. In the lower half of the picture are the regulators and valves that control flow in and out of the five cylinders.

Calibration loads are measured using NIST-traceable load cells with accuracies of ±0.01% f.s. The load cells are Interface Model 1210 full-bridge strain-gage cells. A set of Encore Model 633 strain gage bridge amplifiers provide precision voltage supplies to each cell and amplify the bridge outputs.

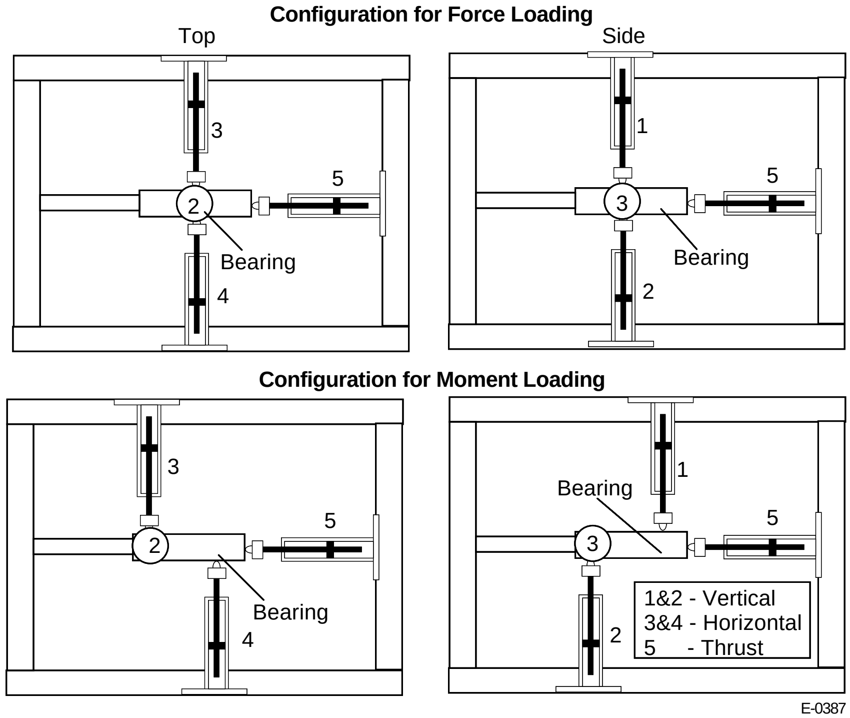

Figure 9. Arrangement of cylinders for load application.

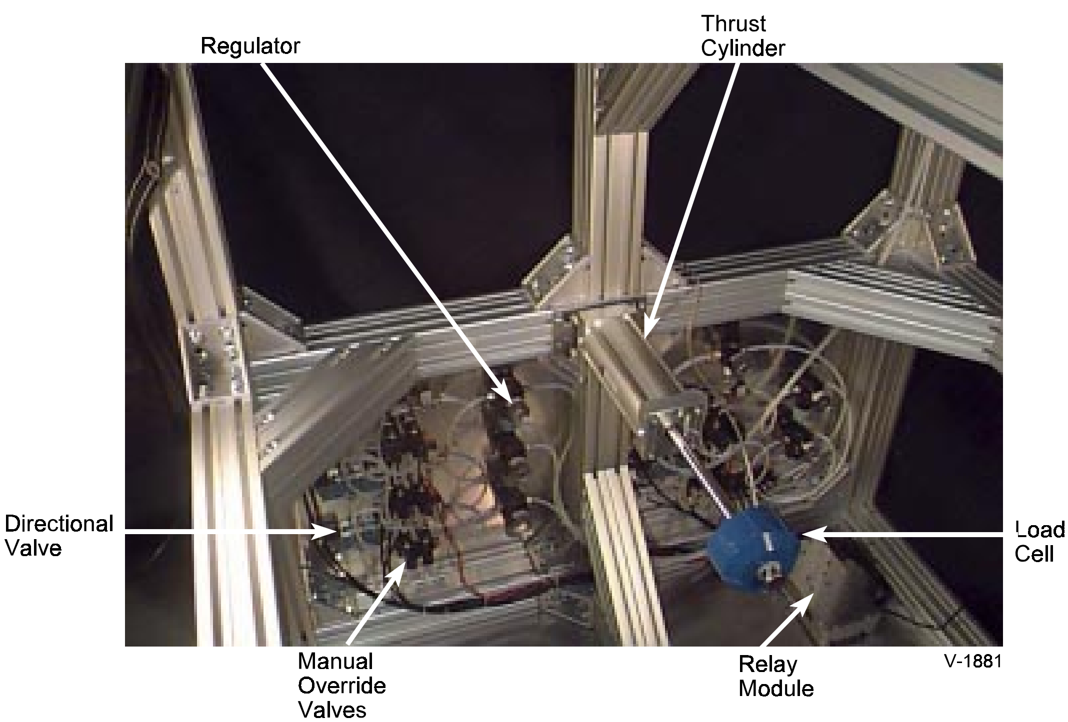

Figure 10. PSI automated calibration rig.

Calibration Results

A preliminary calibration shows that the air bearing balance responds linearly to applied static loads. The bearing was calibrated at a supply pressure of 200 psig, rather than the maximum design pressure of 400 psig. For this condition, the maximum (50% gap deflection) load is 200 lb. Calibrations were performed at several angles as the response of the bearing varies slightly with the angle of the rotating element. The following paragraphs describe the behavior of the various sensors.

Figure 11 shows how the journal bearing sensors respond to a side force. In this test, the load was increased and then decreased through a series of steps, so that hysteresis could be assessed. Note that all sensors show some offset. This is due in part to manufacturing variations around the bearing and, in the case of the lift sensors, due to the weight of the calibration body.

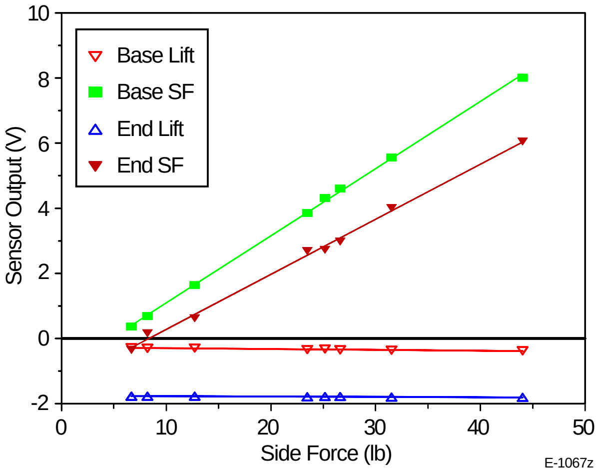

Figure 11. Side force load response of journal bearing sensors.

The horizontal sensors respond linearly to a side-force load. The aggregate linearity and hysteresis error for the sideforce sensors was 0.6% for the base sensor and 1.1% for the end. The vertical sensors show little response to the side load, as expected. The slopes for these sensors were less than 1% of the slope for the horizontal sensors. As shown in Figure 12, the thrust sensors also exhibit little response to the side load.

Figure 13 shows that under large loads, the response to loads is no longer linear. In this plot, a lift sensor shows curvature in its response to an applied lift load. A polynomial fit can be used to improve accuracy in a large-load calibration. Note that although the linear range of the bearing is being exceeded, no damage is

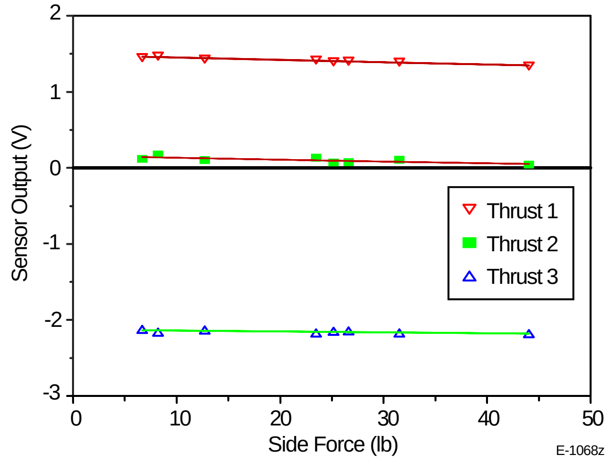

Figure 12. Response of thrust sensors to side loads.

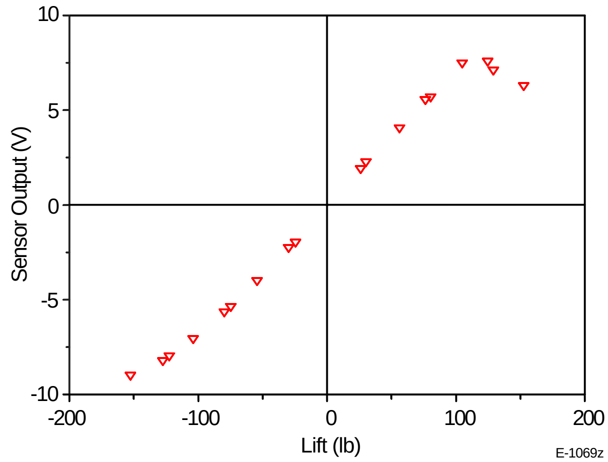

Figure 13. Response of a vertical sensor to over-range lift load. Response is linear but balance is not damaged.

done to the bearing. The deflection is in the air film and not in the sensing element, as is the case for a strain gage balance. At high spin rates, it may be difficult to stabilize the bearing, so large film deflections should be avoided. However, for some cases, it may be useful to extend the range with a nonlinear calibration. On the extreme right side of the plot, the curve changes direction, and the balance is obviously not useful at this extreme.

Figure 14 shows the response of the thrust sensors to an applied thrust load. Again, the response is linear with aggregate linearity and hysteresis errors less than 0.8% full scale for all sensors.

Because the film gap is extemely small, it is difficult to maintain constant nominal gap height for a large

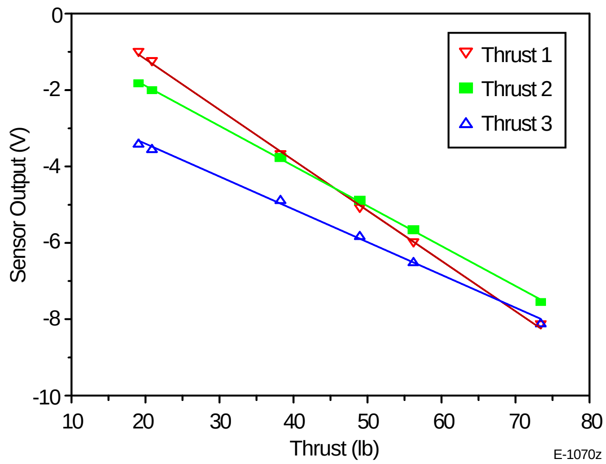

Figure 14. Thrust sensors respond linearly to thrust loads.

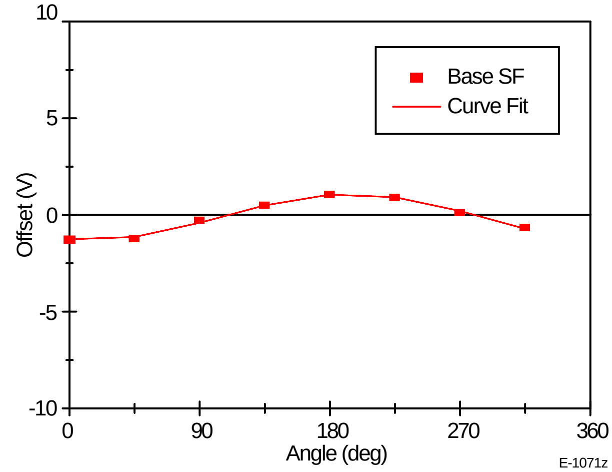

Figure 15. Base horizontal sensor offset voltage varies with angle of rotating element.

bearing like the present subject. Thus, both offset and slope vary with rotor angle. For this reason, the bearing must be calibrated as a function of angle. Figures 15 and 16 show the variation in offset and slope for the base side force sensor. The offset (Figure 15) varies substantially - +/-10% full scale - over one revolution. The slope exhibits smaller variations of about 2% of its value. Both can be fit with sine functions as indicated on these plots. The combined error using this fit, assuming no linearity or hysteresis, would be about 1%. This can be improved if more complex curve fits are used.

The air bearing balance is required to measure loads at high frequencies. The instrumentation module that accepts the sensor signals, computes loads, and transmits them to a wind tunnel data acquisition system, is intended to perform these calculations at 2 kHz. It is necessary, then for simple curve fits to be used. It is possible to build a lookup table and interpolate linearly between points. In its continuation, the development of the air bearing will assess this possibility.

The bearing as well as the calibration system is still under development. It will be possible to improve the linearity and hysteresis errors with some improvements to the cylinder mounting hardware. At present, the cylinders permit some small changes in the angles at which they applied. This motion may contribute to some of the error in calibration and will be eliminated in the continuing work.

Conclusions

An air bearing balance was built to measure loads on spinning test articles in a wind tunnel. The balance is equipped with a brushless motor to impart spin to the bearing. The air bearing provides nearly frictionless

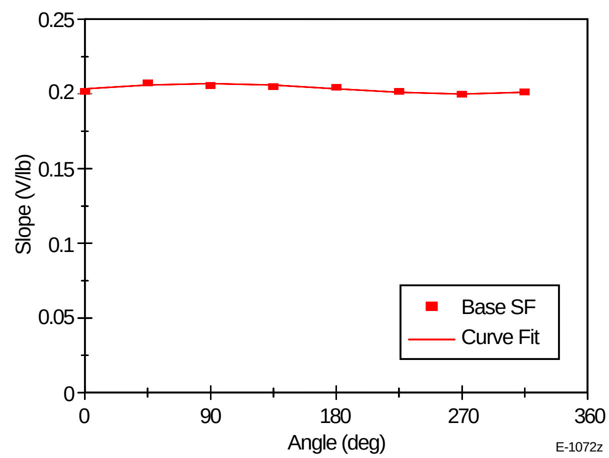

Figure 16. Base horizontal sensor side force sensitivity varies with angle of rotating element.

rotation. Loads are measured by sensing pressure differences across the air bearing film. The device is equipped with an auxiliary air delivery system that may be used to test models requiring air for jets or pneumatic actuators.

Preliminary calibration experiments show that the balance responds linearly to loads up to a 50% deflection of the film gap. The response of sensors to loads off of their primary orientation is small. The calibration constants are functions of rotation angle and hence calibration must be performed at several angles. At present, the calibrations indicate that combined linearity and hysteresis errors less than 1.1% full scale can be achieved.

Tests planned for the future include a study of the effect of spin rate on calibration sensitivity. Frequency response measurements are also needed to fully characterize the balance. The motor torque sensor must be calibrated, and the auxiliary air system must be demonstrated. The balance will be demonstrated in an upcoming wind tunnel test wherein the loads will be measured on a spinning 155 mm projectile.

Acknowledgments

This work is sponsored by Arnold Engineering Development Center, Arnold Air Force Base, TN under the supervision of Ron Bishel. The authors thank Ed Marquart of Sverdrup/AEDC for his valuable input.

References

1. J. Magill, K. McManus, M. Miller, and M. Allen, "A High Bandwidth Air Bearing Balance for Dynamic Wind Tunnel Testing," AIAA 97-3648, AIAA Atmospheric Flight Mechanics Conference, New Orleans, LA, August 11-13, 1997.

2. C.L. Ratliff, E.J. Marquart, An Assessment of a Potential Test Technique:Virtual Flight Testing," AIAA Atmospheric Flight Mechanics Conference, August 7-9, 1995, Baltimore, MD.

3. C.W. Halderman, A.D.Weinberg, "Force Measurement on Rotating Ablating Models Using an Air Bearing Balance," AIAA Journal, Vol. 30, No. 4, April 1992.

4. Burt, G.E., "Design of a Wind Tunnel Roll Damping Balance Incorporating Externally Pressurized Gas Bearings Operating at Large Film Reynolds Numbers," AEDC-TR-69-204, October 1969.

5. Gross, W.A., Gas Film Bearings, 1966.

6. Hamrock, B.J., Fundamentals of Fluid Film Lubrication, McGraw-Hill, NY, 1994.

7. J.H. Vohr, Notes from RPI-MTI Gas Bearing Design Course, Mechanical Technology Inc., Latham, NY, 1966.

8. Roblee, J.W., Design of Externally Pressurized Gas Bearings for Dynamic Applications, Ph.D. Thesis, University of California at Berkeley, 1985.

9. Blondeel, E., Snoeys, R., and DeVrieze, L., "Dynamic Stability of Externally Pressurized Gas Bearings," Journal of Lubrication Technology, Vol. 102, p. 511, October 1980.